

Received: 2016.08.27  
Accepted: 2016.10.10  
Published: 2017.05.07

# Grading of Gliomas by Using Radiomic Features on Multiple Magnetic Resonance Imaging (MRI) Sequences

Authors' Contribution:  
Study Design A  
Data Collection B  
Statistical Analysis C  
Data Interpretation D  
Manuscript Preparation E  
Literature Search F  
Funds Collection G

**BCEF 1 Jiing-bo Qin**  
**B 2 Zhenyu Liu**  
**AG 1 Hui Zhang**  
**C 2 Chen Shen**  
**B 3 Xiao-chun Wang**  
**C 1 Yan Tan**  
**B 2 Shuo Wang**  
**E 1 Xiao-feng Wu**  
**A 2 Jie Tian**

1 Department of Radiology, First Clinical Medical College, Shanxi Medical University, Taiyuan, Shanxi, P.R. China  
2 Key Laboratory of Molecular Imaging, Institute of Automation, Chinese Academy of Sciences, Beijing, P.R. China  
3 Department of Medical Imaging, Shanxi Medical University, Taiyuan, Shanxi, P.R. China

**Corresponding Authors:** Hui Zhang, e-mail: 3160405096@qq.com, Jie Tian, e-mail: jie.tian@iaac.cn  
**Source of support:** This study was supported by grants from the National Natural Science Foundation of China (81471652) to Hui Zhang

**Background:** Gliomas are the most common primary brain neoplasms. Misdiagnosis occurs in glioma grading due to an overlap in conventional MRI manifestations. The aim of the present study was to evaluate the power of radiomic features based on multiple MRI sequences – T2-Weighted-Imaging-FLAIR (FLAIR), T1-Weighted-Imaging-Contrast-Enhanced (T1-CE), and Apparent Diffusion Coefficient (ADC) map – in glioma grading, and to improve the power of glioma grading by combining features.





**Material/Methods:** Sixty-six patients with histopathologically proven gliomas underwent T2-FLAIR and T1WI-CE sequence scanning with some patients (n=63) also undergoing DWI scanning. A total of 114 radiomic features were derived with radiomic methods by using in-house software. All radiomic features were compared between high-grade gliomas (HGGs) and low-grade gliomas (LGGs). Features with significant statistical differences were selected for receiver operating characteristic (ROC) curve analysis. The relationships between significantly different radiomic features and glial fibrillary acidic protein (GFAP) expression were evaluated.

**Results:** A total of 8 radiomic features from 3 MRI sequences displayed significant differences between LGGs and HGGs. FLAIR GLCM Cluster Shade, T1-CE GLCM Entropy, and ADC GLCM Homogeneity were the best features to use in differentiating LGGs and HGGs in each MRI sequence. The combined feature was best able to differentiate LGGs and HGGs, which improved the accuracy of glioma grading compared to the above features in each MRI sequence. A significant correlation was found between GFAP and T1-CE GLCM Entropy, as well as between GFAP and ADC GLCM Homogeneity.

**Conclusions:** The combined radiomic feature had the highest efficacy in distinguishing LGGs from HGGs.

**MeSH Keywords:** **Glioma • Magnetic Resonance Imaging • Multilocus Sequence Typing • Radiometric Dating**

**Full-text PDF:** <http://www.medscimonit.com/abstract/index/idArt/901270>

 3226  —  6  29



## Background

Gliomas are the most common primary brain neoplasms. They are classified into 4 grades (grade I–II, low-grade; grade III–IV, and high-grade) according to the guidelines of the World Health Organization (WHO) [1,2]. The accurate grading of gliomas has clinical significance for therapeutic decision-making, the monitoring and administration of chemoradiotherapy, and prognostic evaluation [3]. Accurate prognostic prediction is required to carry out more personalized treatment of patients. Conventional magnetic resonance imaging (MRI) and apparent diffusion coefficient (ADC) can provide important discerning information for glioma grading [4,5]. However, misdiagnosis occur in glioma grading due to the overlap in conventional MRI manifestations between low-grade (LGGs) and high-grade (HGGs) gliomas [6].

Radiomics is an emerging area that can transform multidimensional image data into the features amenable to comprehensive quantification by using an automatic feature extraction algorithm [7–10]. Radiomics provides a comprehensive quantification of tumors by extracting and mining large numbers of quantitative image features from medical images. Compared with conventional MRI, this technique is a quantitative method providing more detailed quantification of tumor phenotypic characteristics. The results of radiomics are less subject to interference from human-induced factors. Currently, radiomics is used for evaluating the prognosis of lung cancer as well as the clinical phenotype [11–13]. For example, radiomic quantitative features contained a number of important prognostic indicators, including the molecular subtypes of tumors [11]. Despite enormous potential, radiomic techniques have disadvantages in routine clinical practice. First, post-processing technology is complex and requires specialized procedures and software. Second, the post-processing does not yet have a unified standard. Finally, the delineations of ROIs require clinicians to draw layer-by-layer on imaging, which were too complicated and tedious for clinicians.

Previous studies using single-sequence imaging and a single feature were reasonably useful for glioma grading [14–16]. However, a single sequence with a single feature cannot comprehensively incorporate all features of gliomas [17]. Because heterogeneity is an important characteristic of gliomas, using only 1 sequence cannot examine all features of gliomas [14]. For example, an MR image using multi-sequence may display diverse signal characteristic due to the various pathological changes of gliomas, such as hemorrhage, necrosis, and cystic degeneration in tumors. Thus, radiomic features from a multi-sequence MR image may be useful for glioma grading as a promising noninvasive biomarker of malignant tumors.

In the present study, we investigated the efficacy of using radiomic features from multiple MRI sequences (T2-FLAIR, T1WI-CE, and ADC map) in glioma grading. First, we aimed to determine the optimal radiomic features of each sequence and then combined those features to acquire better efficiency in glioma grading. Radiomic features from multiple sequences and combined features may provide more comprehensive information for glioma grading and supplement conventional MRI and other functional MRI features [18,19]. Combined features may supply a frame of reference for clinical diagnosis and treatment decision-making, as well as for prognosis prediction.

## Material and Methods

### Patient selection

This retrospective study was approved by the local institutional review board. Written informed consent was obtained from every patient before participation. A total of 66 patients with gliomas underwent MRI between February 2012 and October 2015. Inclusion criteria were: (a) MR imaging performed in all patients within 2 weeks prior to surgical resection and/or chemoradiotherapy and (b) a histopathologic diagnosis of cerebral glioma and grouped into LGGs and HGGs using the WHO 2007 criteria. DWI images of 3 patients were excluded because they displayed severe movement artifacts. Finally, a total of 66 patients (33 males; 22–73 years of age; mean age 51.5 years) with T2-FLAIR and T1WI-CE sequences, and 63 patients with DWI sequences were included.

### Image data acquisition

MRI examinations were performed with a Signa HDx 3-T MR scanner using an 8-channel phase array head coil (GE Healthcare, Milwaukee, WI). All patients underwent conventional MR sequences axial T1-weighted imaging (T1WI) with a repetition time (ms)/echo time (ms) of 195/4.76 and axial T2-weighted imaging (T2WI) with 4000/98 and T2WI-FLuid Attenuated Inversion Recovery (T2WI-FLAIR) with 8000/95 and an inversion time (TI) of 2371.8 ms. Axial contrast-enhanced T1WI (T1WI-CE) was repeated after intravenous administration of 0.1 mmol/kg of gadolinium contrast with gadopentetate dimeglumine. A total of 63 patients underwent the axial DWI sequence with TR/TE 5000/74. Other MR sequence parameters included slice thickness and slice intervals of 6.0/1.2 mm, while field of view (FOV) was 240×240 mm for all axial sequences. DWI scans used the SE/EPI sequence, and the diffusion coefficient of sensitivity was selected as 0.1000 s/mm<sup>2</sup>. The original DWI maps were transmitted to ADW4.4 (Advanced Workstation 4.4) to generate axial ADC maps using GE software processing.

### Tumor segmentation on image

The MR image of the T2WI-FLAIR, T1WI-CE, and ADC maps were transmitted from the PACS workstation (SiChuang Ltd., Beijing, China) to a personal computer, and then transferred into processable DICOM format images using RadiAnt DICOM Viewer software (available at <http://www.radiantviewer.com>). Owing to heterogeneity of gliomas, 2-dimensional (2-D) regions of interest (ROIs) were delineated manually using opening ITK-SNAP software (available at <http://www.itksnap.org>) by 2-way-blinded, experienced neuroradiologists until they reached an agreement on areas of enhancement in each axial T1 post-contrast MR slice, tumor parenchyma T2-FLAIR, and ADC maps layer-by-layer.

### Radiomics analysis and processing of image data

We calculated radiomic features from MRI raw DICOM images. First, we selected tumor regions on each slice of the MRI series, such that the sub-regions were made into a matrix with "0" and "1" over the series, where "0" indicated non-tumor and "1" indicated tumor. All calculation procedures were implemented on the cube generated by the dot production of the image matrix of the series and the "0-1" matrix of selected regions. The program was developed by Matlab scripts. Relevant radiomic features were calculated and extracted from cubes on the T2WI-FLAIR, T1WI-CE, and ADC maps, respectively.

The process of extracting radiomic features is shown in Figure 1. Radiomic processing produced 114 quantitative image features derived from the Aerts et al. study [11] for 3 MRI sequences.

### Histopathology

Gross total resection was performed in 65 gliomas, and only 1 glioma was partially resected. Surgical specimens were paraffin-embedded after 4% formalin fixation (buffered in phosphate-buffered saline), and 1- $\mu$ m sections were prepared for hematoxylin-eosin (HE) staining. Gliomas were histopathologically classified according to the 2007 WHO central nervous system classification criteria. In addition to histological grading of the tumors, the immunohistochemistry (IHC) index for GFAP was assessed. The tumor parenchyma underwent corresponding paraffin cuts and conventional dewaxing to water, and ABC immunohistochemical staining was performed. Main reagents and instruments included GFAP monoclonal antibody (Dako, Copenhagen, Denmark), ABC kit (Sigma-Aldrich, St. Louis, MO), DAB chromogenic agent (Sigma-Aldrich, St. Louis, MO), and the Digital Scan Scope case scanning system. GFAP staining was located in the cytoplasm and cell processes, and Aperio digital pathology image analysis system (Leica, Frankfurt, Germany) and software Cytoplasmic V2 (Leica, Frankfurt, Germany) using a magnification of 200X were used

to select richly stained tumor tissue sections. Three standard fields of vision were randomly selected and the average optical density was measured 3 times to compute an average for GFAP expression levels of cells.

### Statistical analysis

Statistical analysis was performed using SPSS version 18.0 software. The 2-sample *t* test was used to compare the values of all radiomic features between LGGs and HGGs on the T2WI-FLAIR, T1WI-CE, and ADC map, respectively. We selected the radiomic features that had significant differences between LGGs and HGGs for further analysis using 1-way analysis of variance (ANOVA) with a post hoc test to test for differences among grade II, III, and IV gliomas. ROC curve analysis was conducted to determine the diagnostic power of radiomic features that yielded statistically significant differences between LGGs and HGGs on each sequence in glioma grading. We normalized the features and combined their values to create a new feature (combined feature) to determine whether the efficiency of glioma classification could be increased. Relationships between the radiomic features on each MRI sequence and IHC index of glioma GFAP were analyzed using the Pearson correlation method. For all statistical tests,  $P < 0.05$  was considered statistically significant.

### Radiomic features normalization and combination

The features were normalized for each MRI sequence using the z-score normalization method and the conversion function is displayed in equation (1). The symbols  $\mu$  and  $\sigma$  represent the mean and standard deviation, respectively, of all sample data. The normalized features were then fitted to equation (2) and the combined features were calculated. Here, AUC (area under the ROC curve [AUC]=0.838) and *F* correspond to the area under curve and the value of each feature, respectively.

$$x^* = \frac{x - \mu}{\sigma} \quad (1)$$

$$f(x) = AUC1 * F1 + AUC2 * F2 + \dots + AUCn * Fn \quad (2)$$

## Results

### Comparisons of all values of radiomic features on T2WI-FLAIR, T1WI-CE, and ADC maps between LGGs and HGGs

All the values of radiomic features for different sequences in regions containing gliomas are compared with 2-samples *t* test. We found 2 statistical differential features on T2WI-FLAIR sequence, 3 features on T1WI-CE sequence, and 3 features on the ADC map between LGGs and HGGs ( $P < 0.05$ ). All of the radiomic features that yielded statistically significant differences between

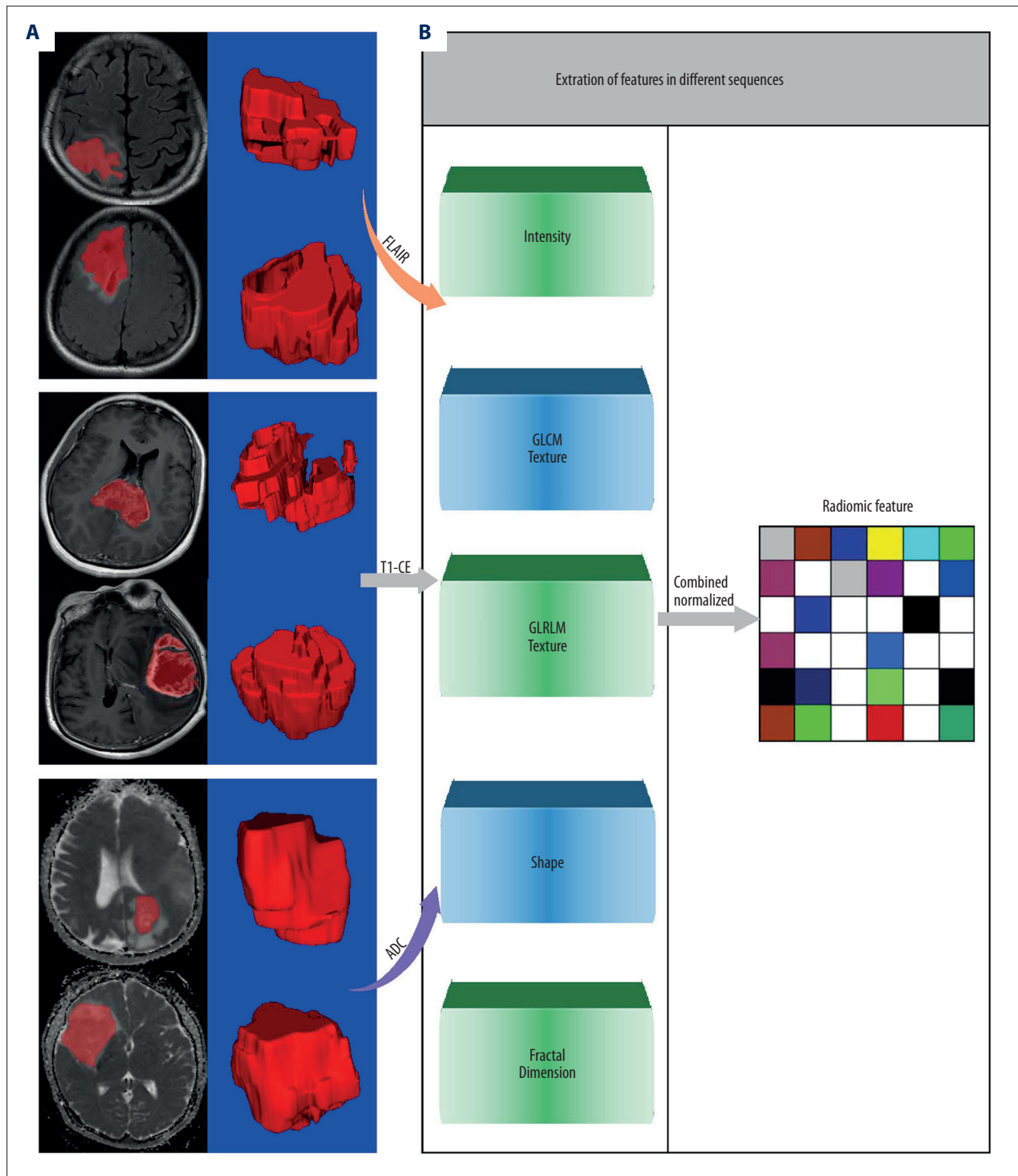


**Figure 1.** Process of extracting radiomic features from MRI images. **(A)** Gliomas are demonstrated on T2WI-FLAIR, T1WI-CE and the ADC map, with MRI profiles (**left**) and 3D visualization model (**right**), respectively. **(B)** To quantify radiomic features, including intensity, texture features based on gray level co-occurrence matrix (GLCM), gray-level run-length matrix (GLRLM), shape, and fractal dimension, were normalized and combined to generate a sketch map of radiomic features.

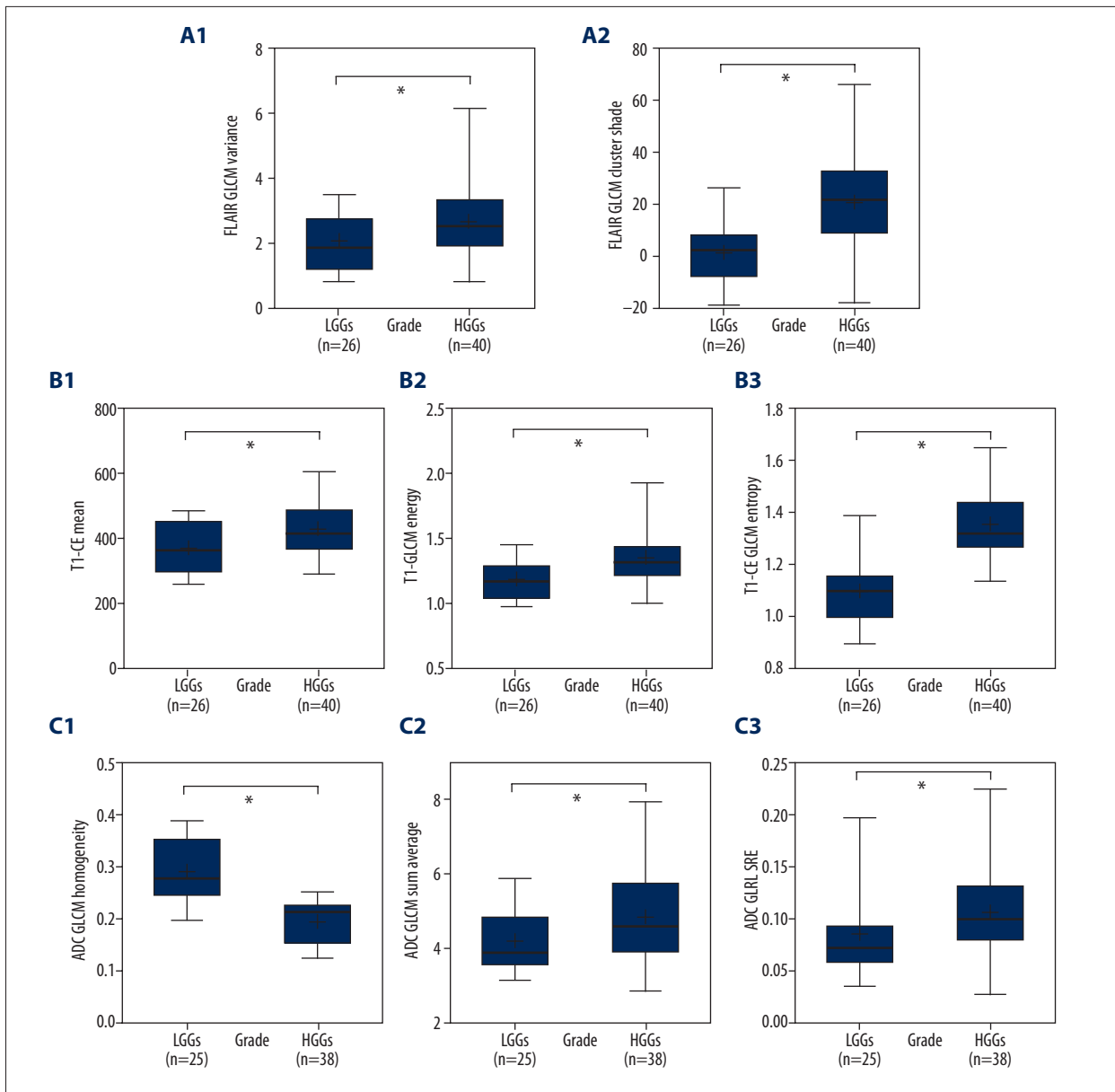


**Figure 2.** Box plots of comparison between LGGs and HGGs for features on 3-MRI sequence. Box plots of radiomic features with statistical differences for LGGs vs. HGGs on the 3 MRI sequences, including FLAIR sequence (**A1**, **A2**), T1-CE sequence (**B1–B3**), ADC map (**C1–C3**). Plus sign (+) represents the mean value of each radiomic feature and asterisk (\*) represents  $P < 0.05$ .

LGGs and HGGs on 3 MRI maps are shown in Figure 2. For example, the feature of FLAIR GLCM Variance was lower in LGGs compared to HGGs ( $2.056 \pm 0.843$  vs.  $2.682 \pm 1.229$ ,  $P = 0.027$ ).

**Comparisons of radiomic features on T2WI-FLAIR, T1WI-CE, and ADC maps among grade II, III, and IV gliomas**

The radiomic features that displayed statistical differences between LGGs and HGGs were further compared using 1-way ANOVA among grade II–IV gliomas. T2WI-FLAIR GLCM Cluster

Shade differed significantly between grades II and III ( $P < 0.001$ ) and between grades II and IV ( $P < 0.001$ ). Only 2 radiomic features, T1WI-CE GLCM Entropy on the T1WI-CE sequence and ADC GLCM Homogeneity on the ADC map, were able to identify gliomas from grades II to IV. Comparisons of the radiomic features among grade II, III, and IV gliomas on T2WI-FLAIR are shown in Figure 3.

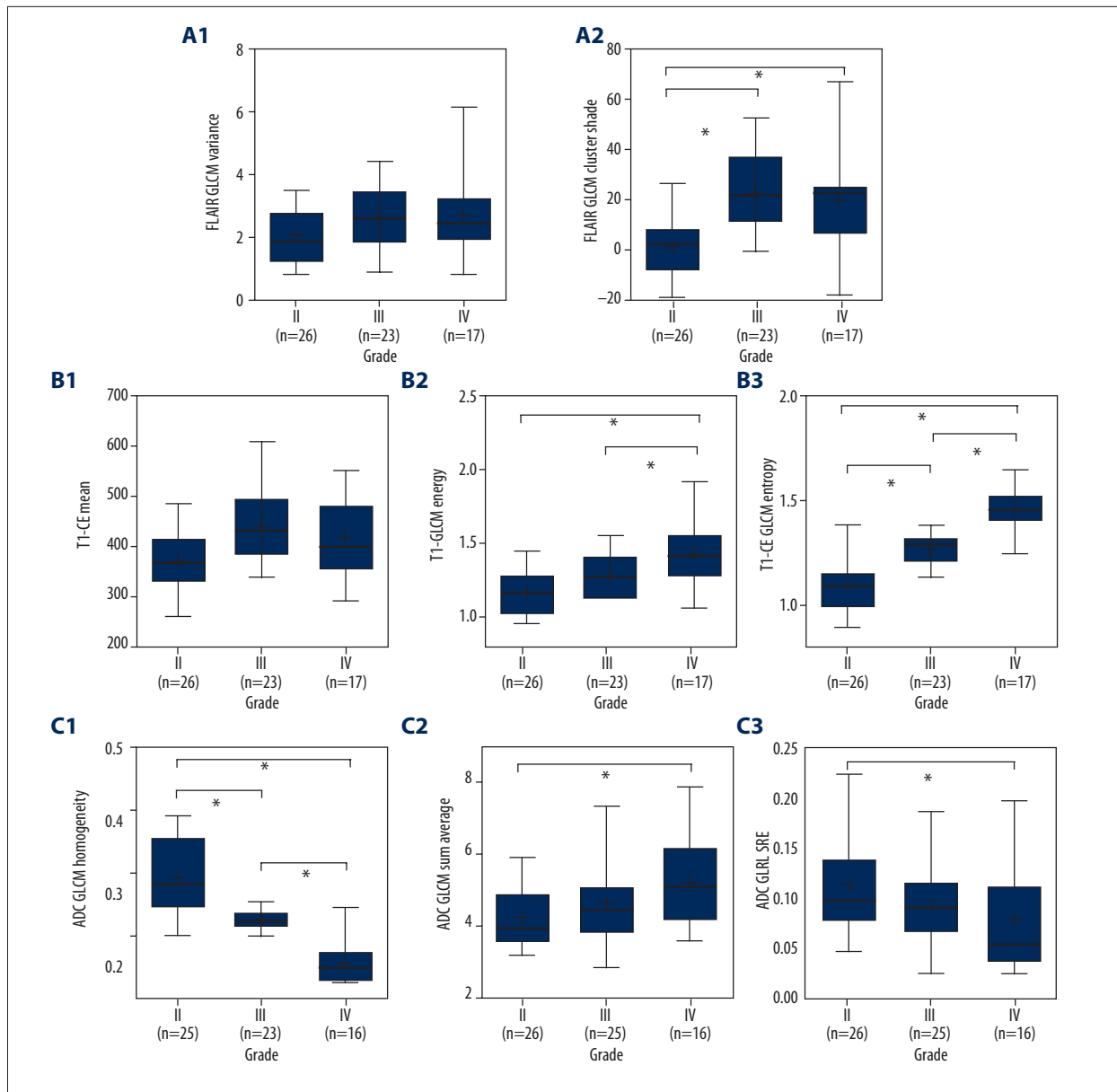


**Figure 3.** Box plots of comparison among grade II–IV gliomas for features on 3-MRI sequence. Box plots of radiomic features with statistical differences for grade II vs. III vs. IV grade on the 3 MRI sequences, including FLAIR sequence (**A1**, **A2**), T1-CE sequence (**B1–B3**), ADC map (**C1–C3**). Plus sign (+) represents the mean value of each radiomic feature and asterisk (\*) represents  $P < 0.05$ .

### ROC analysis of the diagnostic efficiency of radiomic features and the combined feature in differentiating LGGs from HGGs

The diagnostic efficiency of each feature that yielded a statistical difference between LGGs and HGGs was compared using ROC curves, which are shown in Figure 4A–4C. (1) The AUC value of FLAIR GLCM Cluster Shade (0.838), which had high sensitivity (75%) and specificity (84.6%) at a cut-off value of 10.217 ( $P < 0.05$ ), was significantly better than FLAIR GLCM Variance

( $AUC = 0.654$ ) in differentiating LGGs from HGGs. (2) The cut-off value of T1-CE GLCM Entropy (1.176) for distinguishing between LGGs and HGGs had high sensitivity (97.5%) and specificity (80.8%), and the AUC was 0.936 ( $P < 0.05$ ), which was higher than T1-CE Mean ( $AUC = 0.752$ ) and T1-CE GLCM Energy ( $AUC = 0.748$ ). (3) The AUC of ADC GLCM Homogeneity (0.905) which had high sensitivity (97.5%) and specificity (80.8%) at a cut-off value of 1.176 ( $P < 0.05$ ) was significantly better than ADC GLCM Sum Average ( $AUC = 0.684$ ) and ADC GLRL SRE ( $AUC = 0.674$ ) on the ADC map in differentiating LGGs from HGGs.

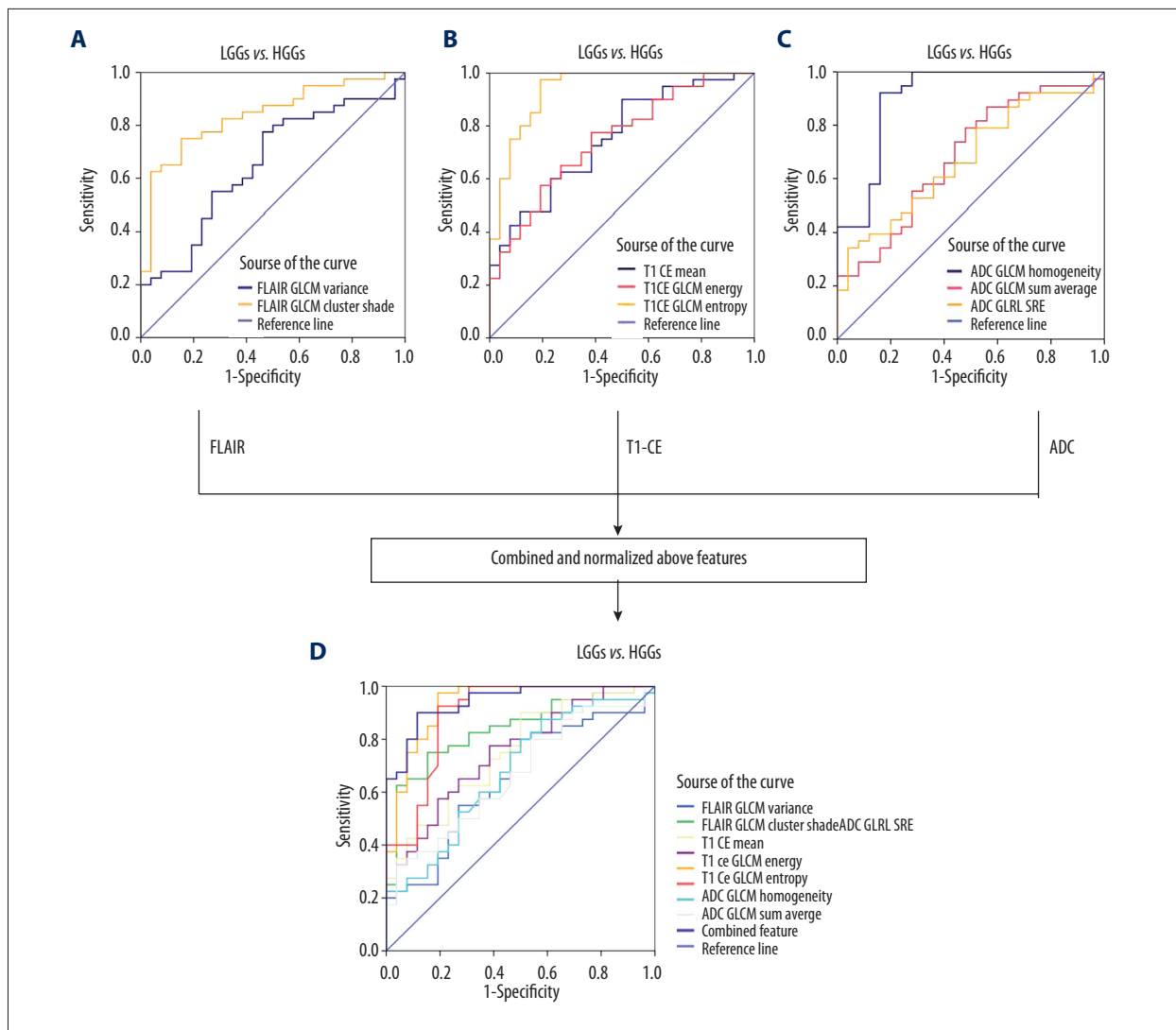


**Figure 4.** ROC curves for radiomic features of 3 sequences and combined feature for differentiating LGGs from HGGs. **(A)** FLAIR GLCM Variance, and FLAIR GLCM Cluster Shade. **(B)** T1-CE Mean, T1-CE GLCM Energy, and T1-CE GLCM Entropy. **(C)** ADC GLCM Homogeneity, ADC GLCM Sum Average. **(D)** ROC curve of combined feature compared with the above features.

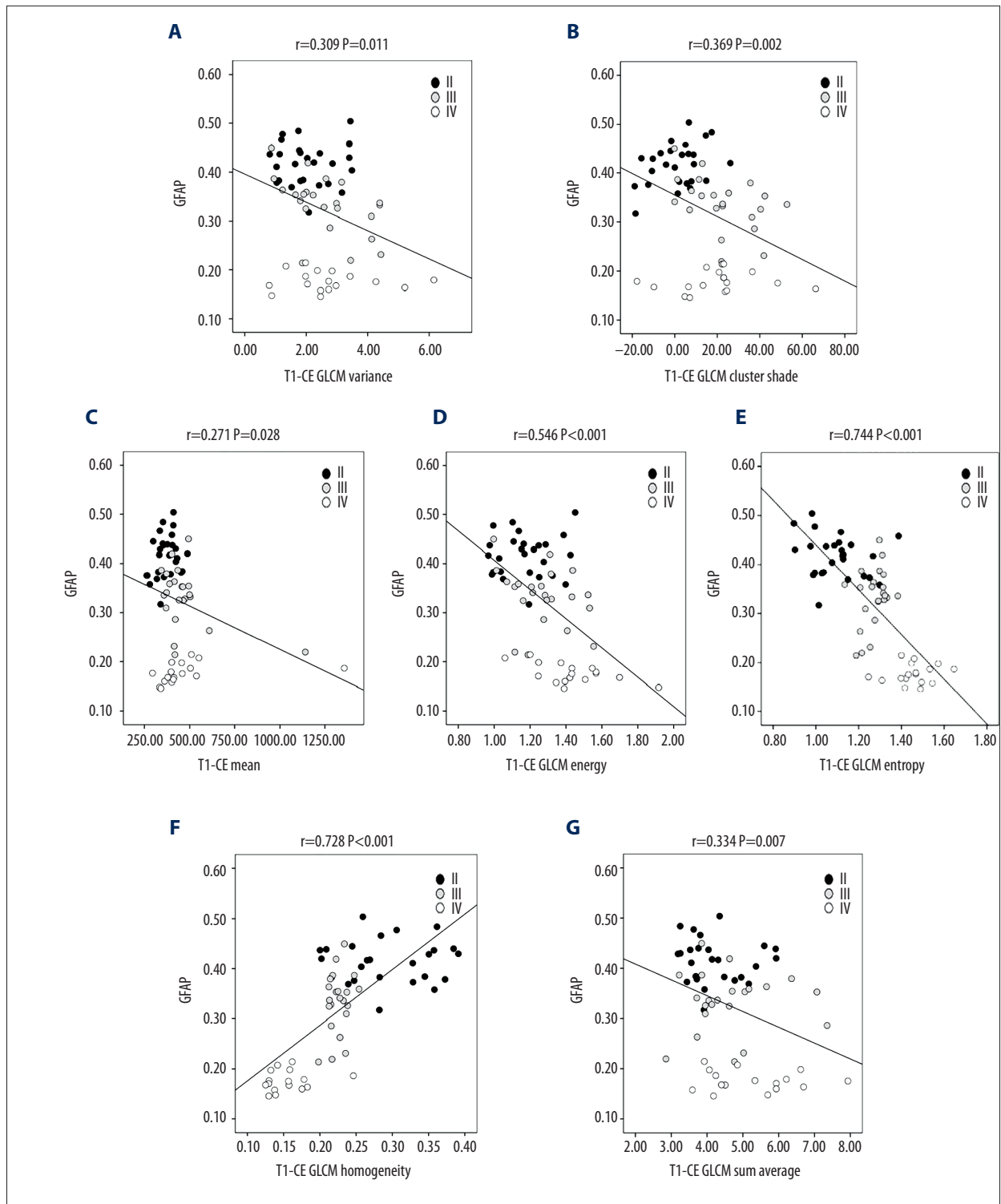
Figure 4D displays ROC curve among the combined feature and above features. The combined feature further increased the diagnostic power, resulting in the highest value of AUC (0.943), higher specificity (89%) compared with T1-CE GLCM Entropy (80.8%), and higher sensitivity (90%) compared to ADC GLCM Homogeneity (84%).

**Correlation between GFAP and radiomic features**

All 66 glioma specimens underwent IHC tests to detect GFAP expression. The prediction of cellular differentiation, invasion and metastasis is valuable in estimating tumor cell biological characteristic, response to therapy, and prognosis. The correlations were evaluated using Pearson correlation analysis between GFAP and each feature, which displayed statistical

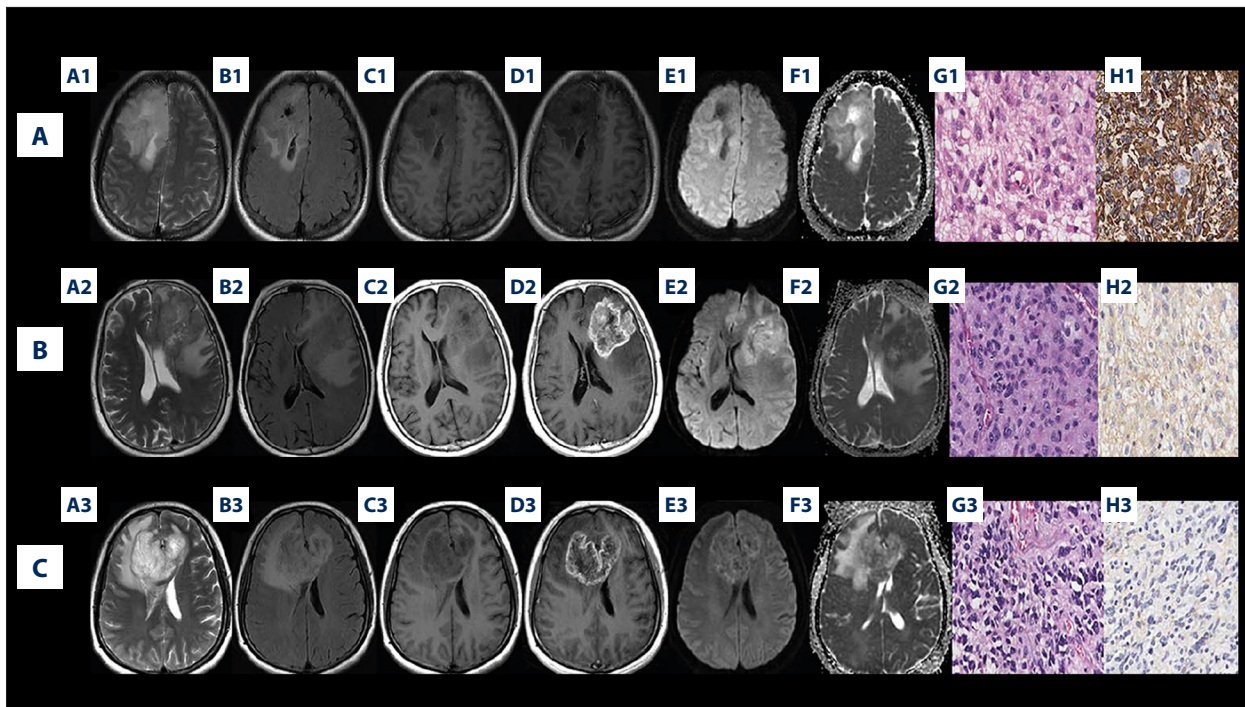
differences between LGGs and HGGs. A significant negative correlation was found between GFAP and the feature T1-CE GLCM Entropy ( $r=-0.744, P<0.001$ ), while a positive correlation was found between GFAP and the feature ADC GLCM Homogeneity ( $r=0.728, P<0.001$ ). In addition, the features of FLAIR GLCM Variance ( $r=-0.309, P=0.011$ ), FLAIR GLCM Cluster Shade ( $r=-0.369, P=0.002$ ), T1-CE GLCM Energy ( $r=-0.546, P<0.001$ ), and ADC GLCM Sum Average ( $r=-0.334, P=0.007$ ) demonstrated negative correlations with GFAP. The corresponding correlation coefficients and scatter plots are shown in Figure 5.

Figure 6 shows representative T2WI, T2-FLAIR, T1WI, T1WI-CE, DWI, ADC maps, pathological HE staining, and IHC GFAP expression for glioma grades II, III, and IV, respectively. GFAP expression decreased with increasing glioma grade.



**Figure 5.** Correlations between GFAP and each radiomic feature on multiple MRI sequences with statistical difference among grade II, III, and IV gliomas.





**Figure 6.** (A) Images of a grade II glioma in the right frontal lobe. (A1) Lesion showed diffused iso-hyperintense signal on T2-weighted image. (B1) T2-FLAIR image displayed diffused iso-hyperintense signal in the parenchyma of the tumor. (C1) T1-weighted image showed iso-hypointense signal. (D1) T1-weighted image with contrast enhancement showed no definitive enhancement. (E1) Diffusion-weighted image showed iso-hypointense signal. (F1) ADC map showed iso-hyperintense signal. (G1) Well-differentiated tumor cells with slight nuclear atypia shown on HE staining map. (H1) High expression of GFAP in the cytoplasm. (B) Images of a grade III glioma in the left frontal lobe. (A2) T2-weighted image showed isointense signal with multiple hyperintense foci in the center of the tumor. (B2) T2 FLAIR image showed isointense signal. (C2) T1-weighted image showed iso-hypointense signal. (D2) T1-weighted image with contrast enhancement displayed moderate enhancement. (E2) Diffusion-weighted image showed hyperintense signal in the lesion. (F2) ADC map showed iso-hypointense signal. (G2) HE staining map showed moderately differentiated tumor cells with nuclear atypia. (H2) Moderate GFAP expression in the cytoplasm. (C) Images of a grade IV glioma in the bilateral frontal lobe and corpus callosum. (A3) T2-weighted image showed hyperintense signal. (B3) T2 FLAIR image displayed iso-hyperintense signal. (C3) T1-weighted image showed hypointense signal. (D3) T1-weighted image with contrast enhancement showed heterogeneous enhancement. (E3) Diffusion-weighted image showed iso-hyperintense signal. (F3) ADC map showed high-low mixed signal. (G3) Poorly differentiated tumor cells with remarkable nuclear atypia were displayed on HE staining map. (H3) Low GFAP expression in the cytoplasm.

## Discussion

In the present study we evaluated the potential of radiomic features based on multiple sequences for use in glioma grading. We then combined features that were able to differentiate between LGGs and HGGs to determine whether diagnostic efficiency could be improved for glioma grading. In addition, we studied the correlation between these radiomic features and GFAP. Our results showed that the features of FLAIR GLCM Cluster Shade, T1-CE GLCM Entropy, and ADC GLCM Homogeneity had high power in differentiating LGGs and HGGs on each MRI sequence. Furthermore, the combined feature improved the diagnostic ability to differentiate LGGs from HGGs. A significant correlation was found between GFAP and the feature T1-CE GLCM Entropy ( $r=0.744$ ,  $P<0.001$ ) and

ADC GLCM Homogeneity ( $r=0.728$ ,  $P<0.001$ ). Thus, combined features from different MRI sequences may serve as an optimal radiomic feature for grading gliomas in clinical practice.

Radiologists can make an accurate diagnosis for the majority of gliomas by using experience, but in some cases different diseases may exhibit the same or similar image features. For instance, the scope of necrosis and signal characteristics of tumors on various MR images may not be visually distinct for radiologists, but after radiomic calculation processes and feature extraction using various algorithms, detailed quantitative feature information may vary to a large extent. Radiomics is an emerging field of research, and has recently become an area of great interest [7]. We hoped to apply radiomics to extract quantitative features for the comprehensive assessment

of gliomas. We found that GLCM Entropy from the T1 CE sequence and GLCM Homogeneity from the ADC map were best able to differentiate the glioma grades.

A previous study by Ryu et al. [16] investigating the ability of texture features on the ADC map to distinguish between HGGs and LGGs demonstrated that entropy of ADC could be used for differentiation and the value of entropy was significantly higher in HGGs than LGGs. In our study, however, GLCM Entropy on the T1 CE sequence displayed high diagnostic efficiency among the different grades of gliomas. The discordance between sequences may be caused by differences between algorithms and the delineation of tumor ROIs between radiologists. Additionally, our finding that entropy value was significantly higher in HGGs than LGGs is consistent with the findings of the previous study. Entropy of texture is an index that has been broadly used for radiomic analysis in previous research [20–22]. When all of the elements in the co-occurrence matrix have the greatest randomness and the elements of the co-occurrence matrix distributes in the dispersion, the value of entropy is large. Entropy represents the non-uniformity or the complexity of the image texture. Therefore, HGLs display high heterogeneity due to multiple tissue elements and MRI shows complex signal changes.

Kang et al. [23] found that the mean ADC values of grade II and III gliomas were lower than grade IV gliomas because of the inclusion of microscopic necrosis regions and the partial volume-averaging effect in measurement. In our study, the value of ADC GLCM Homogeneity was significantly different between various glioma grades. GLCM Homogeneity could reflect the texture homogeneity in images and measure the local variation in texture [24]. The value of GLCM Homogeneity decreased with increased changes in image texture between the different regions. In this study, ADC GLCM Homogeneity values significantly reduced in the high-grade gliomas. Therefore, lower value of ADC GLCM Homogeneity might reflect and explain the internal heterogeneity of malignant gliomas.

In the majority of recent studies employing quantitative image feature assessment for gliomas, only 1 category feature from 1 MRI sequence, such as texture, was applied [16,25], which provided limited information. In this study we investigated the efficiency of radiomic features from multiple MRI sequences for gliomas grading, yielding promising results. We demonstrated the use of radiomic quantitative MRI features on multiple sequences to differentiate between different grades of gliomas. We found that the features of T1-CE GLCM Entropy and ADC GLCM Homogeneity had high potential in differentiating between LGGs and HGGs.

In previous studies, the cumulative histogram was used to distinguish between HGGs and LGGs [23]. However, specific feature

values reflect only partial features of the tumor. In our study we normalized and combined the radiomic features of multiple MRI sequences that significantly differentiated between LGGs and HGGs. The combined feature further increased diagnostic power and had the highest AUC (0.943) and higher specificity (89%) compared with T1-CE GLCM Entropy, as well as higher sensitivity (90%) compared with ADC GLCM Homogeneity after ROC curve analysis. Combining multiple radiomic features improved the ability to differentiate HGGs and LGGs. One possible explanation is that normalized combined radiomics from multiple MRI sequences may take into account the malignance and heterogeneity of gliomas more objectively. Thus, we could non-invasively quantify tumor features better, and provide a new research strategy for glioma grading using the radiomics method.

Temporal and spatial heterogeneity is one of the most significant characteristics of malignant tumors, due to molecular and pathological changes [26]. GFAP is an intermediate filament cytoskeleton protein which is expressed specifically by the gliocyte, with a molecular weight of 51 kDa [27]. Reduced expression of GFAP from neuroglia cells can cause changes that make it more easy for tumor cells to infiltrate surrounding structures [28]. Ilhan-Mutlu et al. [29] reported that decreased GFAP expression was associated with increasing malignancy grade in gliomas. In the present study, significant correlations were revealed between GFAP expression and the features T1-CE GLCM Entropy and ADC-GLCM Homogeneity. We found a significant negative correlation between GFAP and the feature T1-CE GLCM Entropy ( $r=-0.744$ ,  $P<0.001$ ), as well as a positive correlation between GFAP and the feature ADC GLCM Homogeneity ( $r=0.728$ ,  $P<0.001$ ). The decreased GFAP expression correlated with aggressiveness and malignance of gliomas, while entropy reflected spatial irregularity; these could be potential explanations for the negative correlation between T1-CE GLCM Entropy and GFAP expression, as well as the positive correlation between the feature ADC GLCM Homogeneity and GFAP. Increasing the heterogeneity and complexity of the microenvironment in gliomas can result in non-homogeneity of the signal on different MRI sequences. Therefore, cellular karyokinesis, during which cells from gliomas infiltrate surrounding tissue, can be non-invasively evaluated using the features T1-CE CLCM Entropy and ADC GLCM Homogeneity.

There were, however, limitations to this study that must be addressed. First, the patient population was small relatively. Second, ROIs were manually delineated one-by-one on slices, which may lead to variability between radiologists. On the other hand, manually drawing ROIs is a tedious procedure. Finally, our investigation did not involve prognosis analysis, which should be explored in future research.

## Conclusions

In conclusion, radiomic features of T1-CE GLCM Entropy and ADC GLCM Homogeneity based on entire tumor volume can be a useful tool for grading gliomas. The greatest diagnostic efficiency was found for the combined feature for distinguishing LGGs from HGGs. Furthermore, we showed that radiomic features are significantly associated with the underlying molecular phenotype patterns of GFAP. Therefore, our strategy of radiomics provides a noninvasive, convenient, and repeatable method of glioma grading for use in clinical medicine, potentially accelerating the development of personalized medicine.

## References:

- Louis DN, Ohgaki H, Wiestler OD et al: The 2007 WHO classification of tumours of the central nervous system. *Acta Neuropathol*, 2007; 114: 97–109
- Omuro A, DeAngelis LM: Glioblastoma and other malignant gliomas: A clinical review. *JAMA*, 2013; 310: 1842–50
- Ahmed R, Oborski MJ, Hwang M et al: Malignant gliomas: current perspectives in diagnosis, treatment, and early response assessment using advanced quantitative imaging methods. *Cancer Manag Res*, 2014; 6: 149–70
- Kim HS, Kim SY: A prospective study on the added value of pulsed arterial spin-labeling and apparent diffusion coefficients in the grading of gliomas. *Am J Neuroradiol*, 2007; 28: 1693–99
- Bai X, Zhang Y, Liu Y et al: Grading of supratentorial astrocytic tumors by using the difference of ADC value. *Neuroradiology*, 2011; 53: 533–39
- Scott JN, Brasher PM, Sevick RJ et al: How often are nonenhancing supratentorial gliomas malignant? A population study. *Neurology*, 2002; 59: 947–49
- Lambin P, Rios-Velazquez E, Leijenaar R et al: Radiomics: Extracting more information from medical images using advanced feature analysis. *Eur J Cancer*, 2012; 48: 441–46
- Kumar V, Gu Y, Basu S et al: Radiomics: The process and the challenges. *Magn Reson Imaging*, 2012; 30: 1234–48
- Lambin P, van Stiphout RG, Starmans MH et al: Predicting outcomes in radiation oncology – multifactorial decision support systems. *Nat Rev Clin Oncol*, 2013; 10: 27–40
- Parmar C, Rios-Velazquez E et al: Robust Radiomics feature quantification using semiautomatic volumetric segmentation. *PLoS One*, 2014; 9: 1–8
- Aerts HJ, Velazquez ER, Leijenaar RT et al: Decoding tumour phenotype by noninvasive imaging using a quantitative radiomics approach. *Nat Commun*, 2014; 5: 1–8
- Parmar C, Leijenaar RT, Grossmann P et al: Radiomic feature clusters and prognostic signatures specific for Lung and Head & Neck cancer. *Sci Rep*, 2015; 5: 1–10
- Coroller TP, Grossmann P, Hou Y et al: CT-based radiomic signature predicts distant metastasis in lung adenocarcinoma. *Radiother Oncol*, 2015; 114: 345–50
- Brynnolfsson P, Nilsson D, Henriksson R et al: ADC texture – an imaging biomarker for high-grade glioma. *Med Phys*, 2014; 41: 1–7
- Drabycz S, Roldan G, de Robles P et al: An analysis of image texture, tumor location, and MGMT promoter methylation in glioblastoma using magnetic resonance imaging. *Neuroimage*, 2010; 49: 1398–405
- Ryu YJ, Choi SH, Park SJ et al: Glioma: Application of whole-tumor texture analysis of diffusion-weighted imaging for the evaluation of tumor heterogeneity. *PLoS One*, 2014; 9: 1–9
- Lee J, Choi SH, Kim JH et al: Glioma grading using apparent diffusion coefficient map: Application of histogram analysis based on automatic segmentation. *NMR Biomed*, 2014; 27: 1046–52
- Zhang H, Tan Y, Wang XC et al: Susceptibility-weighted imaging: The value in cerebral astrocytomas grading. *Neurol India*, 2013; 61: 389–95
- Wang XC, Zhang H, Tan Y et al: Combined value of susceptibility-weighted and perfusion-weighted imaging in assessing who grade for brain astrocytomas. *J Magn Reson Imaging*, 2014; 39: 1569–74
- Ganeshan B, Skogen K, Pressney I et al: Tumour heterogeneity in oesophageal cancer assessed by CT texture analysis: Preliminary evidence of an association with tumour metabolism, stage, and survival. *Clin Radiol*, 2012; 67: 157–64
- Ng F, Ganeshan B, Kozarski R et al: Assessment of primary colorectal cancer heterogeneity by using whole-tumor texture analysis: Contrast-enhanced CT texture as a biomarker of 5-year survival. *Radiology*, 2013; 266: 177–84
- Win T, Miles KA, Janes SM et al: Tumor heterogeneity and permeability as measured on the CT component of PET/CT predict survival in patients with non-small cell lung cancer. *Clin Cancer Res*, 2013; 19: 3591–99
- Kang Y, Choi SH, Kim YJ et al: Gliomas: Histogram analysis of apparent diffusion coefficient maps with standard- or high-b-value diffusion-weighted MR imaging – correlation with tumor grade. *Radiology*, 2011; 261: 882–90
- Pantic I, Pantic S, Basta-Jovanovic G: Gray level co-occurrence matrix texture analysis of germinal center light zone lymphocyte nuclei: Physiology viewpoint with focus on apoptosis. *Microsc Microanal*, 2012; 18: 470–75
- Rodriguez Gutierrez D, Awwad A, Meijer L et al: Metrics and textural features of MRI diffusion to improve classification of pediatric posterior fossa tumors. *Am J Neuroradiol*, 2014; 35: 1009–15
- Davnull F, Yip CS, Ljungqvist G et al: Assessment of tumor heterogeneity: An emerging imaging tool for clinical practice. *Insights Imaging*, 2012; 3: 573–89
- Husain H, Savage W, Grossman SA et al: Pre- and post-operative plasma glial fibrillary acidic protein levels in patients with newly diagnosed gliomas. *J Neurooncol*, 2012; 109: 123–27
- Elobeid A, Bongcam-Rudloff E, Westermark B, Nister M: Effects of inducible glial fibrillary acidic protein on glioma cell motility and proliferation. *J Neurosci Res*, 2000; 60: 245–56
- Ilhan-Mutlu A, Wagner L, Widhalm G et al: Exploratory investigation of eight circulating plasma markers in brain tumor patients. *Neurosurg Rev*, 2013; 36: 45–55

## Acknowledgements

We would like to acknowledge Dandan Zheng in MR Advanced Application, GE Healthcare Greater China for parameters of MRI setting and manuscript checking.

## Conflict of interest

The authors declare that they have no conflicts of interest concerning this article.